E. van der Heide
e-mail: e.vanderheide@ind.tno.nl
TNO Industrial Technology,
PO Box 6235,
5600 HE, Eindhoven,
The Netherlands

D. J. Schipper
University of Twente,
PO Box 217,
7500 AE, Enschede,
The Netherlands

On the Frictional Heating in Single Summit Contacts: Towards Failure at Asperity Level in Lubricated Systems

The influence of surface roughness and thermal conductivity on seizure in lubricated contacts is described in this work by quantifying the action of individual asperities in relation to local surface temperature rise. Application of the model to a contact situation in metal forming of stainless steel sheet material reveals the importance of a high quality finish in terms of the center line average roughness of the surface. Calculations show that seizure of single summit contacts can be avoided by surfaces with enhanced thermal conductivity. [DOI: 10.1115/1.1645872]

1 Introduction

The relation between seizure in lubricated sliding systems and the temperature at which a tribo system operates is studied extensively. Pin-plate experiments for example, showed that the frictional behavior changes abruptly as a function of the bulk temperature of the system. The critical temperature, T_{cr}, at which this change occurred was influenced by the composition of the lubricant [1]. As friction generates heat, a local rise in temperature or flash temperature, T_f [2], occurs, which has the same negative influence on the performance of a sliding system. Spikes and Cameron [3] proved that failure in lubricated systems at low or moderate sliding velocities is controlled by the degree of coverage of the surface by lubricant molecules. By showing a linear relationship between the logarithm of the concentration and $1/T_{cr}$ for scuffing data, it was demonstrated that failure occurred at a critical coverage. Since the coverage is controlled by the contact temperature, this confirms and refines Blok's postulate of a constant scoring temperature [4]. The effect of surface roughness on lubricant failure is often not incorporated in the presented models, since flash temperature calculations are usually performed with ideally smooth surfaces [5,6]. The objective of this work is to describe the influence of surface roughness, by quantifying the action of individual asperities in relation to lubricant failure. Such an approach would be able to predict the effect of the surface finishing technique like grinding or milling, on the tribological performance in lubricated sliding systems. Furthermore, effort is put in describing the effect of tool material properties on preventing lubricant failure. This subject is of particular importance in sheet metal forming (SMF) processes where the application of enhanced tool surfaces would possibly allow for the introduction of easy-to-clean and environmentally friendlier forming lubricants, without loss of performance [7]. The scope of this work is limited to a specific contact situation, shown in Fig. 1: the sliding contact between a rigid summit and a plastically deforming counter surface, with hardness H. The applied load results into an attack angle θ, or equally to a contact area, a half circle, with radius a_s, as can be seen from Fig. 1. The actual occurring attack angle or contact radius depends on the radius β of the rigid summit as well as the indentation depth.

Contributed by the Tribology Division for publication in the ASME JOURNAL OF TRIBOLOGY. Manuscript received by the Tribology Division January 21, 2003 revised manuscript received July 10, 2003. Associate Editor: L. Chang.

2 Local Surface Temperature Rise

The maximum flash temperature for contacting surfaces with dissimilar thermal conductivity, K, is estimated by Bos and Moes [5,6], based on the quasi-steady state surface temperature distribution of Carslaw and Jeager [8]. By dividing heat sources, of arbitrary shape and distribution, into a set of point sources and integrating the effect of the point sources over the area covered by the heat source, an expression suited for flash temperature calculations in tribological contacts was obtained. For a stationary surface (subscript ''stat'') in sliding contact with a counter surface (subscript ''sliding'') that moves with a velocity v, operating under boundary lubricated conditions, and assuming a semi-ellipsoidal heat source, the flash temperature reads

$$T_f = \frac{f \cdot F_n \cdot v}{\sqrt{ab}} \left(\frac{1}{\frac{K_{\text{stat}}}{0.375 \cdot \Lambda} + \frac{K_{\text{sliding}}}{\vartheta_{\text{sliding}}}} \right) \tag{1}$$

with

$$\vartheta_{\text{sliding}} = \left[(0.375 \cdot \Lambda)^{\lambda} + \left(\frac{0.589}{\sqrt{\left(\phi \cdot \frac{a \cdot v}{\kappa} \right)}} \right)^{\lambda} \right]^{1/\lambda} \tag{2}$$

In which $\kappa = K/(\rho c_p)$ represents the thermal diffusivity of the moving surface; a and b the semi-axes in and perpendicular to the direction of sliding; ϕ is defined as b/a, while the shape factors λ and Λ are defined according to Eq. (3) and Eq. (4).

$$\lambda(\phi) = 0.5 \exp(1 - \phi) - 2.5 \tag{3}$$

$$\Lambda(\phi) = \frac{2\sqrt{\phi}}{1 + \phi\pi} \cdot \frac{2}{\pi} \cdot G\left(\frac{|1 - \phi|}{1 + \phi} \right) \tag{4}$$

$G(n)$ represents the complete elliptic integral of the first kind with modulus n [5]. Similar to [9] one can define an effective thermal conductivity, K_{eff},

$$K_{\text{eff}} = \frac{K_{\text{stat}}}{0.375 \cdot \Lambda} + \frac{K_{\text{sliding}}}{\vartheta_{\text{sliding}}} \tag{5}$$

which rearranges Eq. (1) to Eq. (6), in which F_n represents the normal force and f the coefficient of friction.

$$T_f = \frac{f \cdot F_n \cdot v}{\sqrt{ab} \cdot K_{\text{eff}}} \tag{6}$$

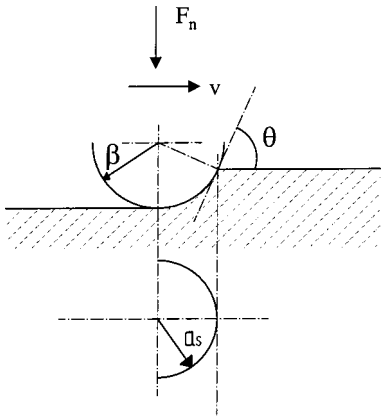

Fig. 1 Sliding contact for a single summit

The solution for surface temperature rise is, although developed for ideally smooth surfaces, applicable to the sliding contact of an individual summit with a plastically deforming counter surface, since no assumptions were made regarding the lateral dimensions of the heat source.

Frictional aspects of single summit contacts are studied in detail by Hokkirigawa and Kato [10]. Experimental evidence for the existence of three wear modes is presented: the cutting mode, the wedge formation mode and the ploughing mode. For each wear mode the coefficient of friction follows from the theoretical work of Challen and Oxley [11]. Furthermore it is shown by [10] that the wear modes can be predicted based upon the attack angle θ and the dimensionless shear strength f_{HK}, see Fig. 2. The latter is defined as the quotient of the interfacial shear stress τ_{int} and the shear strength of the soft metal τ_{soft}.

The transitions are described by the function fits Eq. (7), [12].

$$\theta_{w,pl\to c}=0.25(\pi-\arccos f_{HK}) \quad \theta_{pl\to w}=0.5\arccos f_{HK} \tag{7}$$

An approximate value for f_{HK} in boundary lubricated systems can be found by applying Bowden and Tabor's equation $f=\tau/H$ [13]. In this equation H represents the hardness of the plastically deforming surface and τ the shear strength of the lubricant film. Introducing $f_{HK}=\tau_{\text{int}}/\tau_{\text{soft}}$, $\tau_{\text{int}}=f\cdot H$ and $H=3\sqrt{3}\tau_{\text{soft}}$, yields $f_{\text{HK}}=3\sqrt{3}\cdot f$. Taking 0.08–0.14 as range for f in boundary lubrication (BL), correspond to a f_{HK}-range of 0.4 to 0.7. For each wear mode the amount of heat produced by the sliding action can now be estimated by multiplying the appropriate f with F_n, given by Eq. (8), and the sliding velocity.

$$F_n=\frac{\pi}{2}a_s^2 H \quad \text{with} \quad a_s=\beta\sin\theta \tag{8}$$

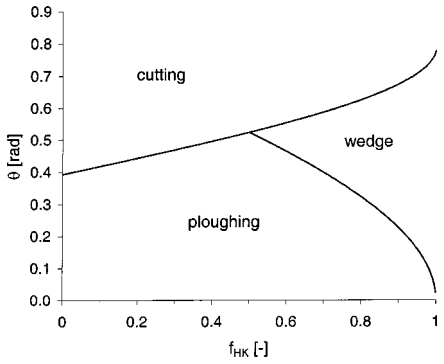

Fig. 2 Wear mode as a function of the dimensionless shear strength f_{HK} and the attack angle θ [10]

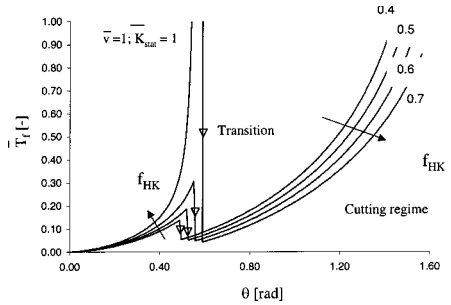

Fig. 3 Nondimensional flash temperature as a function of the attack angle, plotted for f_{HK}-values: 0.4, 0.5, 0.6, and 0.7

Because Eq. (1) is constructed for a semi-ellipsoidally shaped heat source, an equivalent, elliptically shaped contact area is adapted for the contact situation of Fig. 1, with semi-axes a_s and $1/2a_s$, respectively, perpendicular and parallel to the direction of sliding. The Péclet number, Pe, and the resulting normal force are the same for the original and equivalent contact area. The relevant equation for effective thermal conductivity is now given by Eq. (9), with K_{stat} representing the thermal conductivity of the summit and K_{sliding} representing the thermal conductivity of the plastically deforming counter surface ($\phi=2$).

$$K_{\text{eff}}=2.746\cdot K_{\text{stat}}+K_{\text{sliding}}\left[10.379+7.603\cdot\left(\frac{a\cdot v}{\kappa}\right)^{1.158}\right]^{0.432} \tag{9}$$

Optimum similarity analysis [14] of the above equations results into the introduction of seven nondimensional numbers as follows:

$$\begin{gathered}\overline{T_f}=\frac{T_f\cdot\rho_{\text{sliding}}\cdot c_{p,\text{sliding}}}{H} \quad \overline{a_s}=\frac{a_s}{\beta}\\ \overline{F_n}=\frac{F_n}{H\cdot\beta^2} \quad \overline{a}=\frac{a}{\beta}\\ \overline{v}=\frac{v\cdot\rho_{\text{sliding}}\cdot c_{p,\text{sliding}}\cdot\beta}{K_{\text{sliding}}} \quad \overline{K}_{\text{stat}}=\frac{K_{\text{stat}}}{K_{\text{sliding}}}\\ \overline{K}_{\text{eff}}=\frac{K_{\text{eff}}}{K_{\text{sliding}}}\end{gathered} \tag{10}$$

which reduces the set of equations to

$$\begin{gathered}\overline{T_f}=\sqrt{2}\cdot\frac{\overline{F_n}\cdot\overline{v}\cdot f}{\overline{a}\cdot\overline{K}_{\text{eff}}}\\ \overline{F_n}=\frac{\pi}{2}\cdot\overline{a_s}^2\\ \overline{a}=\frac{1}{2}\cdot\overline{a_s}\\ \overline{K}_{\text{eff}}=2.746\cdot\overline{K}_{\text{stat}}+[10.379+7.603\cdot(\overline{v}\cdot\overline{a})^{1.158}]^{0.432}\\ \overline{a_s}=\sin\theta\end{gathered} \tag{11}$$

Based on this set of equations, the flash temperature for a single summit contact can be estimated for a range of material parameters and operational conditions. As an example the flash temperature in its nondimensional form is shown as a function of the attack angle in Fig. 3. It should be noted that part of the curve for $f_{HK}=0.7$ is undefined since no solution for the coefficient of friction is given by the two dimensional slip-line model of [11] for the attack angle range $0.559\leqslant\theta\leqslant0.587$, see appendix A. The calculated nondimensional flash temperature near $f_{HK}=0.559$ be-

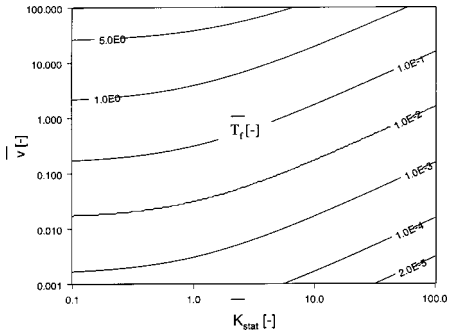

Fig. 4 Effect of the nondimensional conductivity and velocity on the nondimensional flash temperature (θ=0.55, f_{HK}=0.6)

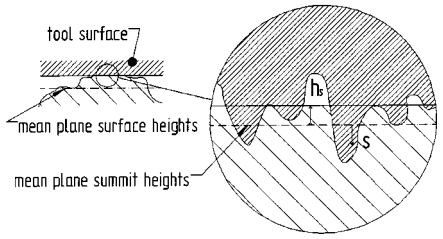

Fig. 5 Multi-asperity contact between a rigid (tool) surface and a plastically deforming (sheet) surface

comes unbounded, which from a physical point of view is hard to imagine. It seems more likely that the flash temperature in single summit contacts is restricted by limits related to the contacting materials, thus introducing a system depended upper limit in Fig. 3. The noncontinuous transition in friction, from ploughing to cutting, and from wedge formation to cutting, causes a clear step in the resulting flash temperature. The sharp reduction in the dimensionless flash temperature, in fact demonstrates that cutting is possible without necessarily increasing the temperature in individual asperity contacts to extremely high values. From Fig. 3 one can conclude that T_f increases with increasing θ and increasing f_{HK} for the ploughing and wedging mode and decreases with f_{HK} in the cutting mode, respectively.

The influence of the nondimensional velocity and the nondimensional conductivity of the summit is as pronounced as the influence of the attack angle. This can be seen from Fig. 4 which represents a severe condition (wedge forming) for a single summit contact. Figure 4 summarizes to a certain extent the influence of the material properties of the contacting surfaces on the resulting flash temperature. Although it is of little use in general engineering practise, since its contour lines depend on the exact combination of f_{HK} and θ, some interesting conclusions can be drawn, which are applicable to more general conditions. First of all it is important to note that the flash temperature is proportional to the hardness of the plastically deforming surface. Materials with approximately the same diffusivity and used under the same contact conditions, which differ by a factor of two in hardness will also differ by a factor of two in flash temperature. The derived proportionality is limited to rigid-plastic single summit contacts, where elastic deformation can be neglected.

Secondly, a modest increase in dimensionless conductivity of the rigid summit causes a significant decrease in flash temperature. The influence of the dimensionless conductivity introduces the possibility to lower the maximum occurring flash temperature to acceptable values, e.g., by application of surface coatings with high thermal conductivity or bulk materials with high conductivity. The nondimensional velocity as applied in Fig. 3 can be interpreted as a Pe-number for a sliding contact at asperity level, taking the summit radius as characteristic length. Figure 4 shows that for both the high and low Pe-regimes there is a distinct influence of the nondimensional conductivity.

3 Application to Engineering Surfaces

The single summit model described in the previous section can be extended to multi-summit, engineering surfaces by integrating the contribution of individual asperities over the total amount of interacting asperities. First a summit needs to be defined. Consider a matrix of asperities heights $z_{i,j}$ with a lateral resolution r_x for the x-direction (rows of the matrix) and r_y in the y-direction (columns of the matrix). An asperity $z_{i,j}$ is regarded as a summit when all eight surrounding neighbors have lower height than $z_{i,j}$. The neighbors on the diagonals are taken into account to prevent saddle-points to be assigned as summit. Knowing the position of the summits allows for representing the summits of a rigid surface by its probability height distribution with standard deviation R_q. Dividing the number of summits by the measured area gives the summit density. A separation h_s, defined as the separation between the mean plane of the summits and the counter surface is used, to calculate the number of summits in contact with the counter surface and the depth of penetration of individual summits, see the right-hand part of Fig. 5. Unlike the model of [15], which assumes equal radii for all summits, from the view point of assessing the wear mode of a summit in contact, it is necessary to calculate the individual summit radii.

An individual radius is calculated for the x and y-direction separately using Eq. (12) [15]:

$$\beta x_{i,j} = -\frac{r_x^2}{z_{i-1,j} - 2z_{i,j} + z_{i+1,j}}$$
$$\beta y_{i,j} = -\frac{r_y^2}{z_{i,j-1} - 2z_{i,j} + z_{i,j+1}} \tag{12}$$

Instead of taking the commonly chosen mean of the radii, the alternative square root of the radii's product is selected as the effective summit radius. Thus,

$$\beta_{i,j} = \sqrt{\beta x_{i,j} \cdot \beta y_{i,j}} \tag{13}$$

The problem of scale change from a single summit model, depicted in Fig. 1, to a multi-summit surface depicted in Fig. 4, can be reduced in determining the geometry and the appropriate attack angle, for each individual summit in contact with the plastically deforming counter surface. The latter is done by [16], showing that Eq. (14) relates the attack angle θ for an individual summit to the height of the summit, s, the separation of the mean summit plane and the counter surface h_s, and the summit's radius β. Now the local surface temperature rise, that takes the complete set of summits into account, can be calculated, using the single summit model.

$$\theta = \begin{cases} \arctan\left(\dfrac{\sqrt{(s-h_s)(2\beta+h_s-s)}}{\beta+h_s-s}\right) & \text{if } s-h_s<\beta \\ \dfrac{\pi}{2} & \text{if } s-h_s \geqslant \beta \end{cases} \tag{14}$$

4 Results

The applicability of the model to engineering surfaces is demonstrated for a tribo system which is of particular interest in sheet metal forming operations, i.e., the sliding contact between tool steel and stainless steel sheet material, in the presence of a boundary lubricant. In sheet metal forming, a hard and smooth tool surface is in sliding contact with a relative soft and rough sheet material. The sheet material will be plastically deformed by applying normal force on the tool-sheet system, which will cause smoothening of the sheet's roughness. A close look at the contact between the smooth roughness plateau's on the sheet and the tool surface, reveals the contact situation of Fig. 5: Contact between

Table 1 Input for flash temperature calculations

Symbol	Value	Unit
f_{HK}	0.6	···
v	0.5	m/s
T_{bulk}	22	°C
K_{stat}	20	$Wm^{-1}K^{-1}$
$K_{sliding}$	16	$Wm^{-1}K^{-1}$
$\kappa_{sliding}$	$4.7\cdot10^{-6}$	m^2/s
H	1.8	GPa

rigid tool summits and a plastically deformed roughness plateau at the sheet surface. Sheet metal forming of stainless steel is known to be sensitive for galling [17], a specific type of sliding wear, which has a direct and negative influence on the lifetime of forming tools and on the surface quality of the products made. The sliding velocity for this contact was taken 0.5 m/s, the bulk temperature of the sheet 22°C (see Table 1). The summit's height distribution of the stationary, rigid surface (the tool), were drawn from standardised Rugotest surfaces produced by Roch Suisse, resulting from planing (no. 101), milling (no. 103), surface grinding (no. 104) and spark erosion (no. 107). Roughness measurements were performed using an interference microscope, of which a full description is given in [12]. The roughness measurements covered an area of 0.149 mm^2, using a pixel size of respectively 1.49 μm in the x-direction and 1.45 μm in y-direction. Results with respect to the standard deviation of the summit's height, R_q, are given in Table 2. Clearly R_q increases with increasing R_a roughness. Especially spark erosion gives rise to high R_q values when compared to the other surfaces at 1.6 and 0.8 μm R_a values. The summit density differs from surface to surface but falls within the range of $2.4-4.4\cdot10^{10}$ per square meter.

The application of Eq. (14) on the summit data set, assuming a separation h_s of $-3R_q$, resulted in a β-θ relations as plotted in Fig. 6, for the ground surfaces. The presented relations are based on function fits, using the power-law function. From Fig. 6 it shows that an increase in R_a shifts the curve to a higher β level, without changing the general relation between the attack angle and the summit's radius. This behavior is also found for the surfaces made by planing, spark erosion and milling. An increase in R_a results, in terms of the presented model, in a higher attack

Table 2 Standard deviation (R_q) of the tool summits height [μm]

R_a [μm]	Planing	Milling	Grinding	Spark erosion
1.6	1.877	1.977	1.878	2.960
0.8	1.106	1.006	1.030	1.352
0.4	···	0.425	0.752	0.746
0.2	···	···	0.339	···
0.1	···	···	0.246	···
0.05	···	···	0.162	···
0.025	···	···	0.021	···

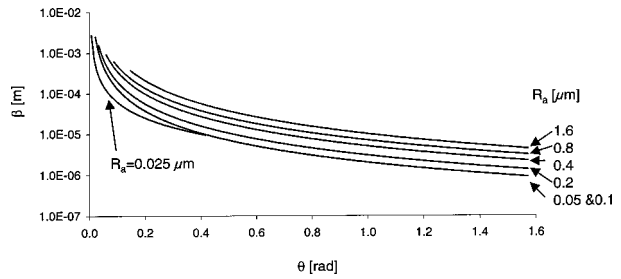

Fig. 6 Summit radius as a function of the attack angle for the ground surfaces

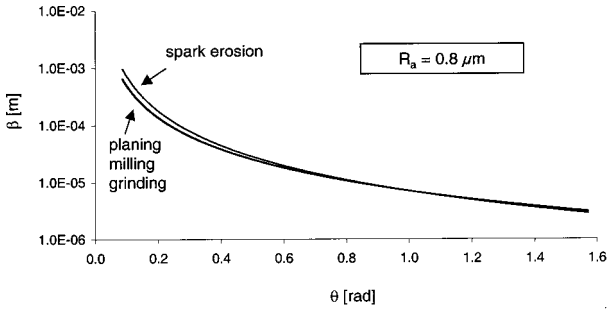

Fig. 7 Summit radius as a function of the attack angle for the surfaces with $R_a=0.8$ μm

angle for a certain summit's radius or equally, the radius of the summit at a certain attack angle value, changes to a higher value. The latter directly affects the value of the dimensionless velocity in Eq. 10, which in turn results in a higher nondimensional flash temperature for a given attack angle (see Fig. 4). From Fig. 7 it shows that the general relation between the summit's radius and the attack angle is hardly affected by the type of surface finish. Spark erosion gave rise to a slightly different curve for the larger summit radii. The smaller radii coincide with the data for the surfaces made by planing, milling and grinding.

The sum of the bulk temperature T_{bulk} and the local surface temperature rise is given in Fig. 8, in case a ground tool surface is selected at $R_a=0.8$ μm. Each dot in this graph represents the calculated T_f for a single summit contact. The three possible wear modes ploughing, wedging and cutting are indicated in this figure by respectively pl, w, and c. Clearly the transition from cutting to wedge formation can be seen from this figure, by the steep step in flash temperature. The transition from ploughing to wedge formation is less visible, since there is no discontinuity in the coefficient of friction for this transition. The attack angle range where wedge formation is expected is of particular interest, since material transfer from the plastically deforming material (sheet) to the rigid surface (tool) will occur for nonlubricated conditions [12]. Such a situation arises if the lubricant film in a single summit contact fails as a result of a local surface temperature that exceeds the critical temperature T_{cr} of the lubricant. The local surface temperature consists of the sum of the bulk temperature and the flash temperature. For applications in SMF seizure of single summit contacts will initiate galling.

Based on the calculated T_f values in Fig. 8, it is not likely that a ground tool surface at $R_a=0.8$ μm can prevent galling. In fact tool life is expected to be short with such a finish. Surface grinding at $R_a=0.05$ μm, however, results in a substantially improved flash temperature distribution, which is given in Fig. 9. The wedge forming summits operate at a temperature level of about 120°C. Now galling could be prevented by heavy duty forming lubricants with a critical temperature above 120°C. The flash temperatures in

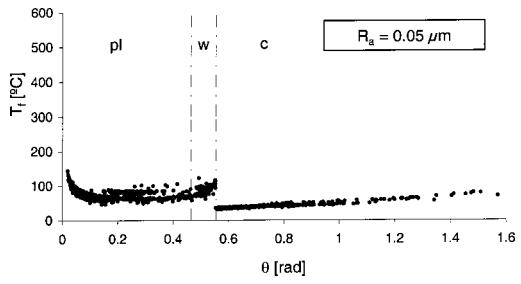

Fig. 8 Flash temperature as a function of the attack angle for the $R_a=0.8$ μm, ground surface. The calculations are made based upon the input given in Table 1.

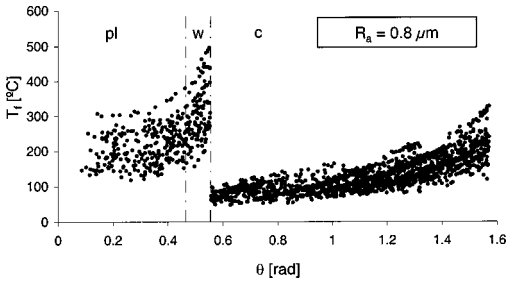

Fig. 9 Flash temperature as a function of the attack angle for the R_a=0.05 μm, ground surface. The calculations are made based upon the input given in Table 1.

single summit contact can be minimized by the application of (tool) surfaces with enhanced thermal conductivity. Figure 10 shows the maximum local surface temperature rise for a single summit contact as a function of the thermal conductivity of the stationary (tool) surface, given the above mentioned tribo system. The drawn lines represent the data for the ground surfaces, the number indicates the R_a roughness. From Fig. 10 it shows that the application of tool materials with enhanced thermal conductivity like 90WC-10Co (K_{stat}=112 W/m·K [18]) would lower the flash temperatures considerably in sliding contact with stainless steel sheet material, when compared with conventional tools steel (K_{stat}=20–30 W/m·K 19). Surfaces with a K_{stat} of about 400 W/m·K would even allow for the introduction of easy-to-clean, light duty forming lubricants, like a solution of 1% stearic acid in white oil (T_{cr}=53°C [1]).

5 Conclusions

A flash temperature model, developed for ideally smooth surfaces, is extended to the contact of a hard rigid summit and plastically deforming material. From calculations it follows that the flash temperature is proportional to the hardness of the plastically deforming material. Materials with approximately the same diffusivity and used under the same contact conditions, which differ by a factor of two in hardness will also differ by a factor two in flash temperature. Secondly, it is shown that a modest increase in dimensionless conductivity of the rigid summit causes a significant decrease in flash temperature.

Application of the model to a contact situation in metal forming of stainless steel sheet material, reveals the importance of a high quality tool finish in terms of the R_a roughness of the surface. Calculations show that seizure of single summit contacts is likely to occur with surfaces made by planing, spark erosion, milling and grinding at an R_a value of 0.8 μm. As a consequence galling is initiated which in turn limits the lifetime of the tools. Reducing the R_a value to 0.05 μm clearly enhances the expected behavior, by reducing the flash temperature for the wedge forming summits to lower values. The flash temperatures in single summit contact can be minimized by the application of tools with enhanced thermal conductivity. It is shown that the application of tools with a thermal conductivity above 400 W/m·K would allow for the introduction of easy-to-clean light duty forming lubricants.

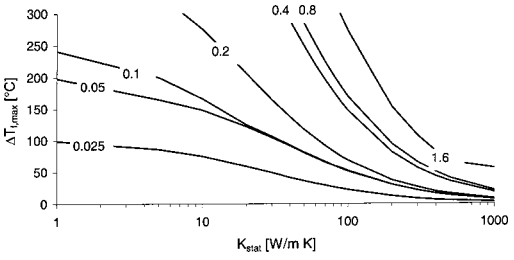

Fig. 10 Maximum local surface temperature rise as a function of the conductivity and of the R_a roughness (surface grinding, Rugotest 104) of the stationary surface

Nomenclature

a = semi-axis contact ellipse in direction of sliding, [m]
a_s = contact radius in summit-sheet contact, [m]
b = semi-axis contact ellipse perpendicular to sliding direction, [m]
c_p = specific heat, [J kg^{-1} K^{-1}]
f = coefficient of friction, [−]
f_{HK} = dimensionless shear strength ($\tau_{\text{int}}/\tau_{\text{soft}}$), [−]
h_s = separation between summit mean plane and mean plane of contacting surface, [m]
r_x = lateral resolution in x-direction, [m]
r_y = lateral resolution in y-direction, [m]
s = summit height, [m]
v = sliding velocity, [m s^{-1}]
$z_{i,j}$ = surface height at position (i,j), [m]
F_n = normal force, [N]
$G(n)$ = complete elliptic integral of the first kind with modulus n, [−]
H = hardness, [Pa]
K = thermal conductivity, [W m^{-1} K^{-1}]
K_{eff} = effective thermal conductivity, [W m^{-1} K^{-1}]
K_{stat} = thermal conductivity of the stationary surface, [W m^{-1} K^{-1}]
K_{sliding} = thermal conductivity of the sliding surface, [W m^{-1} K^{-1}]
Pe = Pe-number (av/κ), [−]
R_a = center line average roughness, [m]
R_q = standard deviation of the profile, [m]
T_{bulk} = bulk temperature, [°C]
T_f = flash temperature, [°C]
T_{cr} = critical temperature of the lubricant, [°C]
β = summit radius, [m]
$\vartheta_{\text{sliding}}$ = auxiliary temperature factor, [−]
θ = attack angle, [rad]
κ = thermal diffusivity ($\kappa=K/\rho c_p$), [m^2 s^{-1}]
λ, Λ = shape factors, [−]
ρ = density, [kg m^{-3}]
τ = shear strength, [Pa]
τ_{int} = interfacial shear strength, [Pa]
τ_{soft} = shear strength soft metal, [Pa]
ϕ = contact aspect ratio b/a, [−]

Abbreviations

c = cutting mode
pl = ploughing mode
w = wedge formation mode
BL = Boundary lubrication
SMF = Sheet metal forming

Appendix A

Coefficient of Friction. Equations (A.1)–(A.3) represent the coefficient of friction f for the three wear modes cutting, ploughing and wedge formation [10,11], respectively

$$f_c=\tan\left(\theta-\frac{\pi}{4}+\frac{1}{2}\arccos f_{HK}\right) \tag{A.1}$$

$$f_{pl}=\frac{\xi_2\sin\theta+\cos(\arccos f_{HK}-\theta)}{\xi_2\cos\theta+\sin(\arccos f_{HK}-\theta)} \tag{A.2}$$

$$f_w=\frac{(1-2\sin\xi_1+\sqrt{1-f_{HK}^2})\cdot\sin\theta+f_{HK}\cos\theta}{(1-2\sin\xi_1+\sqrt{1-f_{HK}^2})\cdot\cos\theta-f_{HK}\sin\theta} \tag{A.3}$$

with

$$\xi_1 = \theta - \frac{\pi}{4} - \frac{1}{2}\arccos f_{HK} + \arcsin\left(\frac{\sin\theta}{\sqrt{1-f_{HK}}}\right) \quad \text{(A.4)}$$

$$\xi_2 = 1 + \frac{\pi}{2} + \arccos f_{HK} - 2\theta - 2\arcsin\left(\frac{\sin\theta}{\sqrt{1-f_{HK}}}\right) \quad \text{(A.5)}$$

The equations derived by [11] are based on two dimensional models and slip-line field theory and provide solutions for the complete ploughing and cutting regime. However, at wedge forming conditions a solution is found only for the (f_{HK}, θ) range, bounded by the conditions of (A.6)

$$(1 - 2\sin\xi_1 + \sqrt{1-f_{HK}^2}) \cdot \cos\theta - f_{HK}\sin\theta > 0 \quad \text{and} \quad \theta \geqslant 0.25(\pi - \arccos f_{HK}) \quad \text{(A.6)}$$

Hence, at $f_{HK} = 0.7$, a condition used in Fig. 3, the coefficient of friction is not defined for the attack angle range $0.559 \leqslant \theta \leqslant 0.587$, which is less than 2 percent of the full attack angle scale $0 - \pi/2$.

References

[1] Frewing, J. J., 1943, "The Heat of Adsorption of Long-Chain Compounds and Their Effect on Boundary Lubrication," Proc. R. Soc. London, Ser. A, **182**, pp. 270–285.

[2] Blok, H., 1963, "The Flash Temperature Concept," Wear, **6**, pp. 483–494.

[3] Spikes, H. A., and Cameron, A., 1973, "Scuffing as a Desorption Process—An Explanation of the Borsoff Effect," ASLE Trans., **17**(2), pp. 92–96.

[4] Blok, H., 1969, "The Postulate About the Constancy of Scoring Temperature, in Interdisciplinary Approach to Friction and Wear," in *Interdisciplinary Approach to the Lubrication of Concentrated Contacts*, P. M. Ku, ed., NASA SP-237, pp. 153–248.

[5] Bos, J., 1995, "Frictional Heating of Tribological Contacts," Ph.D. thesis, University of Twente, Enschede, The Netherlands.

[6] Bos, J., and Moes, H., 1995, "Frictional Heating of Tribological Contacts," ASME J. Tribol., **117**, pp. 171–177.

[7] van der Heide, E., 2002, "Lubricant Failure in Sheet Metal Forming Processes," Ph.D thesis University of Twente, Enschede, The Netherlands.

[8] Carslaw, H. S., and Jeager, J. C., 1959, *Conduction of Heat in Solids*, Oxford University Press, Oxford.

[9] Metselaar, H. S. C., Kerwijk, B., Mulder, E. J., Verweij, H., and Schipper, D. J., 2002, "Wear of Ceramics Due to Thermal Stress: A Thermal Severity Parameter," Wear, **249**, pp. 962–970.

[10] Hokkirigawa, K., and Kato, K., 1988, "An Experimental and Theoretical Investigation of Ploughing, Cutting and Wedge Formation During Abrasive Wear," Tribol. Int., **21**(1), pp. 51–57.

[11] Challen, J. M., and Oxley, P. L. B., 1979, "An Explanation of the Different Regimes of Friction and Wear Using Asperity Deformation Models," Wear, **53**, pp. 229–243.

[12] Rooij, M. B. de, 1998, "Tribological Aspects of Unlubricated Deepdrawing Processes," Ph.D. thesis, University of Twente, Enschede, The Netherlands.

[13] Bowden, F. P., and Tabor, D., 1950, *The Friction and Lubrication of Solids*, Claredon Press, Oxford University Press, Oxford, UK.

[14] Moes, H., 1992, "Optimum Similarity Analysis With Applications to Elastohydrodynamic Lubrication," Wear, **159**, pp. 57–66.

[15] Greenwood, J. A., and Willamson, J. B. P., 1966, "Contact of Nominally Flat Surfaces," Proc. R. Soc. London, Ser. A, **295**, pp. 300–319.

[16] Xie, Y., and Williams, J. A., 1996, "The Prediction of Friction and Wear When a Soft Surface Slides Against a Harder Rough Surface," Wear, **196**, pp. 21–34.

[17] Andreasen, J. L., Eriksen M., and Bay, N., 1997, "Major Process Parameters Affecting Limits of Lubrication in Deep Drawing of Stainless Steel," *Proceedings of the 1st International Conference on Tribology in Manufacturing Processes '97*, K. Dohda, T. Nakamura, and W. R. D. Wilson, eds., Gifu University, Gifu, Japan, pp. 122–127.

[18] Glaeser, W. A., 1992, *Materials for Tribology*, Tribology series 20, Elsevier, Amsterdam.